Kidney International, Vol. 61 (2002), pp. 516–524

Selectins mediate macrophage infiltration in obstructive nephropathy in newborn mice[1]

Bärbel Lange-Sperandio, Francois Cachat, Barbara A. Thornhill, and Robert L. Chevalier

Department of Pediatrics, University of Virginia, Charlottesville, Virginia, USA

Selectins mediate macrophage infiltration in obstructive nephropathy in newborn mice.

Background. Urinary tract obstruction during development leads to tubular atrophy and causes interstitial fibrosis. Macrophage infiltration into the interstitium plays a central role in this process. Selectins, a family of three adhesion molecules, are involved in leukocyte recruitment to sites of inflammation and immune activity. We investigated the role of selectins in obstructive nephropathy in newborn mice.

Methods. Triple selectin-deficient mice ($EPL^{-/-}$), L-selectin deficient mice ($L^{-/-}$) and wild type mice (WT) were subjected to complete unilateral ureteral obstruction (UUO) or sham operation within the first 48 hours of life, and were sacrificed 5 and 12 days later. Kidneys were removed, and sections were stained for macrophage infiltration (mAb F4/80), apoptosis (TUNEL), tubular atrophy (periodic acid-Schiff) and interstitial fibrosis (Masson trichrome).

Results. Selectin deficient mice showed a marked reduction in macrophage infiltration into the obstructed kidney compared to WT at day 5 and day 12 after UUO. Tubular apoptosis was strongly reduced in $EPL^{-/-}$ at day 5 after UUO, and in $EPL^{-/-}$ and $L^{-/-}$ at day 12 after UUO when compared to WT. The number of apoptotic tubular cells was correlated with macrophage infiltration, suggesting that macrophages stimulate tubular apoptosis in obstructive nephropathy. In addition, tubular atrophy and interstitial fibrosis were significantly diminished in $EPL^{-/-}$ and $L^{-/-}$ compared to WT at day 12 after UUO.

Conclusion. Following UUO, selectins mediate macrophage infiltration into the obstructed kidney, which in turn may induce tubular apoptosis, tubular atrophy and interstitial fibrosis.

Obstructive nephropathy is a primary cause of kidney failure in infants and children [1]. Chronic unilateral ureteral obstruction (UUO) leads to interstitial inflammation, interstitial fibrosis and tubular atrophy [2]. Central to these events is the florid macrophage infiltration of the tubulointerstitium, which is preceded by interstitial and tubular up-regulation of macrophage chemokines and adhesion molecules [3–10]. Renal interstitial macrophage infiltration increases as early as 4 to 12 hours after ureteral obstruction and continues to increase over the course of days thereafter [4]. The signal for renal leukocyte recruitment in UUO is macrophage-specific because there are few T lymphocytes noted and an absence of polymorphonuclear leukocytes [11, 12]. Although kidney resident macrophages exist, most macrophages found in the UUO kidney are recruited from the blood vessel system [4, 5]. Macrophages contribute to the tubulointerstitial injury by releasing cytotoxic substances (such as proteolytic enzymes, reactive oxygen radicals, proinflammatory and profibrogenic cytokines) and by activating interstitial fibroblasts [5, 13]. By contrast, lymphocyte infiltration is not required for progressive tubular atrophy and increased interstitial fibrosis in mice with UUO [14]. Although the presence of macrophages within the interstitium in UUO is well established, the mechanisms involved in the recruitment of these immune cells are still poorly defined.

The recruitment of leukocytes from the circulation, and their subsequent influx into surrounding tissues at sites of inflammation or injury is a multistep process that is regulated in part by the selectin family of adhesion molecules [15]. There are three different selectins: E-selectin is expressed on endothelial cells, P-selectin on endothelial cells and platelets, and L-selectin on leukocytes. Whereas E-selectin expression is induced by inflammatory cytokines, P-selectin is rapidly mobilized to the surface of activated endothelium or platelets. L-selectin is constitutively expressed on most leukocytes. Selectins and their ligands mediate the initial contact between circulating leukocytes and the vascular endothelium resulting in capture and rolling of leukocytes along the vessel wall [16, 17]. While rolling, the leukocyte becomes exposed to chemoattractants and activating stimuli expressed on the endo-

[1] **See Editorial by Kipari and Hughes, p. 760.**

Key words: unilateral ureteral obstruction, apoptosis, developing kidney, tubulointerstitial disease, tubular atrophy, interstitial fibrosis, adhesion molecule.

Received for publication July 13, 2001
and in revised form September 24, 2001
Accepted for publication September 25, 2001

thelial surface, which in turn leads to firm adhesion and transendothelial migration, mediated by integrins and their ligands.

Some chemokines and adhesion molecules participating in the leukocyte adhesion cascade have been studied in UUO. Monocyte chemoattractant protein-1 (MCP-1) has been shown to mediate monocyte infiltration following UUO [3]. Intercellular adhesion molecule-1 (ICAM-1) and vascular cell adhesion molecule-1 (VCAM-1) are highly up-regulated on tubular and interstitial cells in the obstructed kidney [8]. Osteopontin, an adhesive protein, mediates macrophage infiltration and interstitial fibrosis in UUO [9]. For the selectin-family of adhesion molecules, it has been reported, that blocking of L-selectin function by a neutralizing antibody was protective against monocyte infiltration after UUO in rats [18]. E- and P-selectin have not been investigated so far. Intravital microscopy studies in gene targeted mice deficient in either E-, P- or L-selectin or various combinations have revealed both overlapping and unique functions of the selectins [19]. Mice with null mutations at individual selectin loci have mild to moderate inflammatory defects, with the severity of defects being $EPL^{-/-} > L^{-/-} > P^{-/-} > E^{-/-}$ [19]. Leukocyte recruitment in triple selectin-deficient $EPL^{-/-}$ mice is significantly impaired [19]. $L^{-/-}$ mice show marked reductions of leukocyte recruitment in several models of inflammation [20–22].

Because most nephrons are formed postnatally in mice, renal development in the neonatal mouse is analogous to renal development in the human fetus. For this reason, surgical ligation of one ureter in newborn mice is a model to study effects of urinary tract obstruction on renal development. The present study was designed to characterize the role of selectins in UUO in newborn mice with null mutation for L-selectin and with triple null mutation for E-, P-, and L-selectin.

METHODS

Experimental protocol

$EPL^{-/-}$ mice, deficient for E-, P-, and L-selectin, as recently described [23], were kindly provided by Dr. A. Beaudet (Baylor College, Houston, TX, USA). L-selectin–deficient mice ($L^{-/-}$) were kindly provided by Dr. T. Tedder (Duke University, NC, USA) [20]. Mutant mice were back-crossed into a C57BL/6 background for at least six generations and maintained in specific pathogen-free conditions. Selectin-deficiency was confirmed by polymerase chain reaction. Wild-type mice of the same genetic background (C57BL/6) were used as controls. Forty-eight hours after birth, male and female mice were subjected to complete left ureteral obstruction ($N = 12$) or a sham operation ($N = 12$) under general anesthesia with isoflurane and oxygen. With the aid of a Wild M3Z stereomicroscope (Leica, Heerbrugg, Switzerland), the distal ureter was exposed through a longitudinal 5-mm left abdominal incision and ligated twice with a 6-0 silk suture (but not transected). In sham operations, the ureter was exposed and repositioned without further manipulation. The incision was closed in a single layer and coated with collodion. After recovery in an oxygen chamber, neonatal mice were returned to their mothers until sacrifice 5 and 12 days after surgery (7 and 14 days of age). The experimental protocol was approved by the Ethics Review Commitee for Animal Experimentation of the University of Virginia.

Identification and quantitation of infiltrating monocytes/macrophages

Infiltration of monocytes/macrophages was examined by immunohistochemistry as described before [24]. Briefly, formalin-fixed, paraffin-embedded sections were deparaffinized, and endogenous peroxidase was inactivated with 0.3% hydrogen peroxide. Sections were then washed in phosphate-buffered saline (PBS) three times, five minutes each, preincubated in a blocking solution (10% goat serum in PBS) for 20 minutes, washed in PBS three times, and then incubated overnight at 4°C with monoclonal F4/80 (supernatant from F4/80 hybridoma cells; ATCC, Manassas, VA, USA), diluted 1:200, as the primary antibody against mouse monocytes/macrophages. Control sections were treated similarly but without addition of the primary antibody. Each section was washed three times in PBS and then incubated with the secondary antibody for 30 minutes. Biotinylated goat anti-rat IgG (Southern Biotechnology Associates, Inc., Birmingham, AL, USA) was used as the second antibody. After the sections were washed with PBS three times, they were incubated for 30 minutes with ABC reagent, containing a preformed avidin and biotinylated horseradish peroxidase macromolecular complex (Vectastain; Vector Laboratories, Burlingame, CA, USA). Each section was washed three times in PBS and then placed in diaminobenzidine/hydrogen peroxide solution, counterstained with methylene blue, dehydrated, and enclosed in an xylene-based mounting medium (Cytoseal XYL; Stephens Scientific, Kalamazoo, MI, USA). Digital images of the sections were superimposed on a grid, and the number of grid points overlapping dark brown macrophages in cortex and medulla was recorded for each field. Twelve nonoverlapping fields at ×400 magnification were analyzed in a blinded fashion. Data were expressed as the mean score ± SE per 12 high power fields. Representative photomicrographs of macrophage infiltration are shown in Figure 1 A and B.

Detection of apoptosis

Apoptotic cells were detected by the terminal deoxynucleotidyl transferase (TdT)–mediated dUTP-biotin nick end labeling (TUNEL) assay as previously described

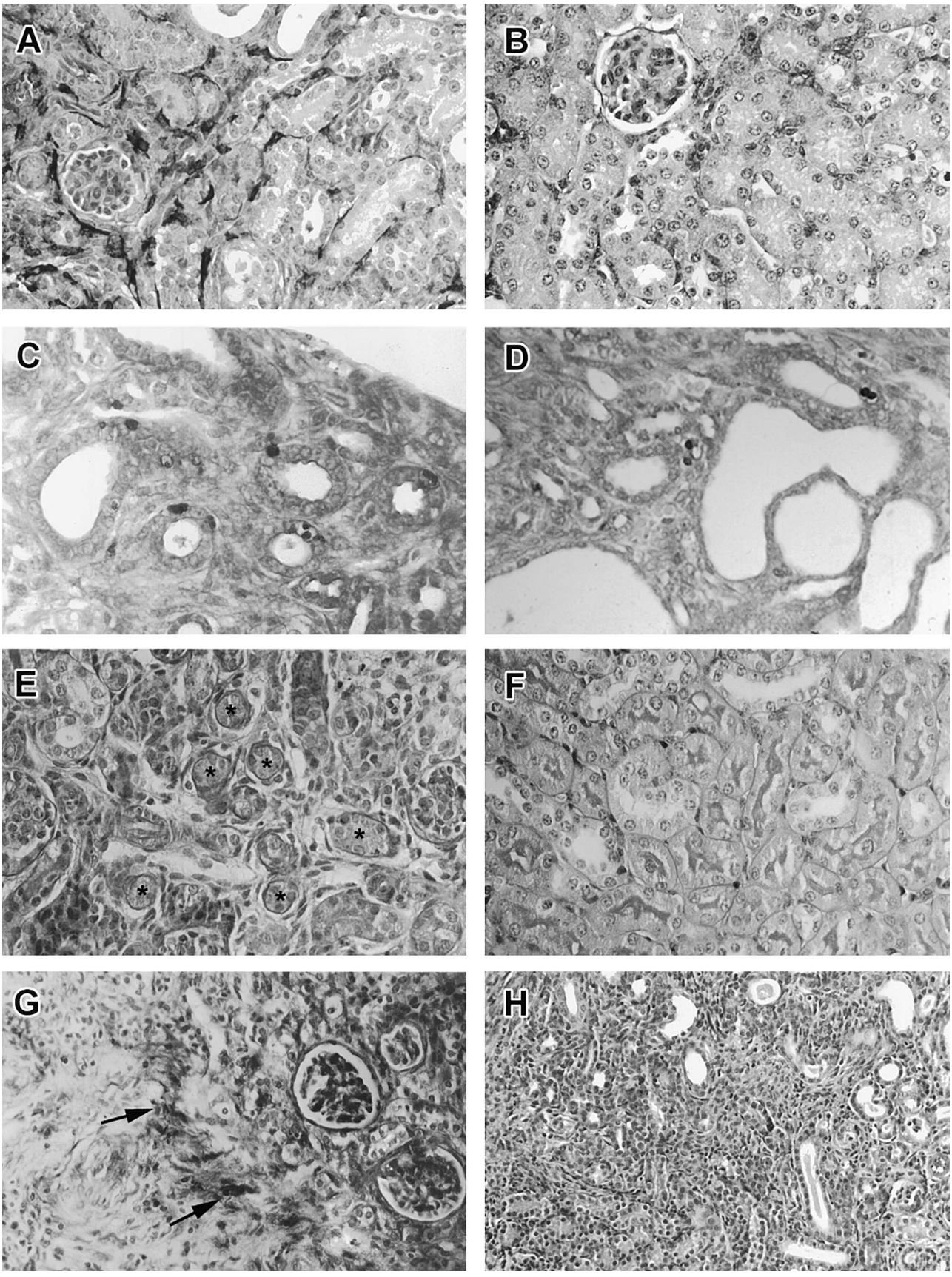

Fig. 1. Representative photomicrographs of obstructed kidneys (UUO). Macrophage infiltration (F4/80 antibody) at twelve days after UUO in control mice (*A*) and in selectin deficient $EPL^{-/-}$ mice (*B*) (magnification ×400). Wild-type mice show interstitial F4/80 positive (black) macrophages (A). $EPL^{-/-}$ kidneys show less macrophages (B). Tubular apoptosis (TUNEL) at five days after obstruction in control mice (*C*) and selectin deficient $EPL^{-/-}$ mice (*D*) (magnification of ×400). $EPL^{-/-}$ kidneys show less TUNEL positive tubular cells. Tubular atrophy (PAS stain) at twelve days after UUO in control mice (*E*) and in selectin deficient mice (*F*) (magnification ×400). Interstitial fibrosis (Masson Trichrome) at twelve days after UUO in control mice (*G*) and in selectin-deficient mice (*H*) (magnification of ×400 and ×250, respectively).

[25]. Briefly, 5-μm formalin-fixed tissue sections were deparaffinized and rehydrated in ethanol followed by incubation with proteinase K (20 μg/mL). After quenching, equilibration buffer was applied, followed by working strength enzyme at a concentration of 1:5 in reaction buffer for one hour at 37°C (ApopTag Peroxidase In Situ Apoptosis Detection Kit; Intergen, Purchase, NY, USA). Cells were regarded as TUNEL positive if their nuclei were stained brown and displayed typical apoptotic morphology with chromatin condensation. The number of TUNEL positive cells in each kidney was calculated in a blinded fashion by counting the number of TUNEL positive tubular cells in 20 sequentially selected fields of renal cortex and medulla at ×400 magnification and expressed as the mean number ± SE per 20 high-power fields. Representative photomicrographs of tubular apoptosis are shown in Figure 1 C and D.

Measurement of tubular atrophy

Kidney sections were stained with periodic-acid Schiff (PAS) for assessment of tubular basement membranes, and tubular atrophy was determined as described previously [26]. Atrophic tubules were identified by their thickened and sometimes duplicated basement membranes. The number of atrophic tubules per field at ×400 magnification was counted, and 20 fields/kidney were analyzed. Representative photomicrographs of tubular atrophy are shown in Figure 1 E and F.

Morphometric evaluation of the interstitial fibrosis of renal cortex

Interstitial collagen deposition was measured in Masson trichrome-stained sections as described before [27]. Digital images of the sections were superimposed on a grid, and the number of grid points overlapping interstitial blue-staining collagen was recorded for each field. Twelve non-overlapping fields at ×400 magnification were analyzed in a blinded fashion. Representative photomicrographs of interstitial fibrosis are shown in Figure 1 G and H.

Statistical analysis

Data are presented as mean ± standard error. Comparisons between groups were made using one-way analysis of variance (ANOVA) followed by the Student-Newman-Keuls test. Comparisons between left and right kidneys were performed using the Student *t* test for paired data. Statistical significance was defined as $P < 0.05$.

RESULTS

Kidney morphology in $EPL^{-/-}$ and $L^{-/-}$ mice

$EPL^{-/-}$ and $L^{-/-}$ mice appeared healthy and developed without apparent defects. The kidneys from the $EPL^{-/-}$ and $L^{-/-}$ mutants were grossly similar to those from wild-type mice. Light microscopic examinations of the kidney showed normal structure of the kidney, that is, glomeruli, tubulointerstitium, and blood vessels (not shown). In obstructed kidneys, there was no difference in histologic parameters between deeper nephrons and newer nephrons on the surface in $EPL^{-/-}$ versus wild-type mice. Renal function tests (urine protein concentration measured by the amidoschwartz method) were normal.

Monocyte/macrophage recruitment

Unilateral ureteral obstruction (UUO) resulted in a significant and progressive increase in interstitial macrophage infiltration in all obstructed wild-type, $EPL^{-/-}$, and $L^{-/-}$ kidneys at all time points studied when compared to sham operated controls and unobstructed intact opposite kidneys (Fig. 2). Selectin-deficient mice showed a significant decrease in interstitial macrophage infiltration into the obstructed kidney when compared to wild-type; $EPL^{-/-}$ demonstrated a decrease by 56% and $L^{-/-}$ showed a decrease by 32% at day 5 after UUO ($P < 0.004$ and $P < 0.02$, respectively). At 12 days after UUO, $EPL^{-/-}$ demonstrated a decrease by 35% and $L^{-/-}$ showed a decrease by 38% ($P < 0.002$ and $P < 0.002$, respectively). No increase in interstitial macrophage infiltration was noted in the contralateral (intact) kidneys in either $EPL^{-/-}$ or $L^{-/-}$ or wild-type mice with UUO at all time points studied.

Tubular apoptosis

Tubular apoptosis was significantly increased in all obstructed kidneys when compared to intact opposite kidneys at day 5 and 12 after UUO (Fig. 3). Interestingly, $EPL^{-/-}$ mice showed a significant decrease in tubular apoptosis when compared to wild-type at day 5 and 12 after surgery. Tubular apoptosis in the obstructed $EPL^{-/-}$ kidney decreased by 47% at day 5 and by 45% at day 12 after UUO when compared to wild-type ($P < 0.005$ and $P < 0.001$, respectively). $L^{-/-}$ mice showed a decrease in tubular apoptosis by 25% at day 5, which was not significant. However, at day 12 after UUO, tubular apoptosis in the obstructed kidney decreased by 43% in $L^{-/-}$ mice when compared to wild-type ($P < 0.001$). A significant correlation ($r = 0.74$, $P < 0.001$) was found between the infiltration of macrophages and the number of apoptotic tubular cells (Fig. 4).

Tubular atrophy

Tubular atrophy in the obstructed kidney was detectable as early as 5 days after UUO (Fig. 5). At 12 days after UUO, there was a dramatic increase in thickened and sometimes duplicated tubular basement membranes in wild-type mice. In contrast, $EPL^{-/-}$ mice showed a significant decrease of tubular atrophy by 57% compared to wild-type. $L^{-/-}$ mice demonstrated a significant de-

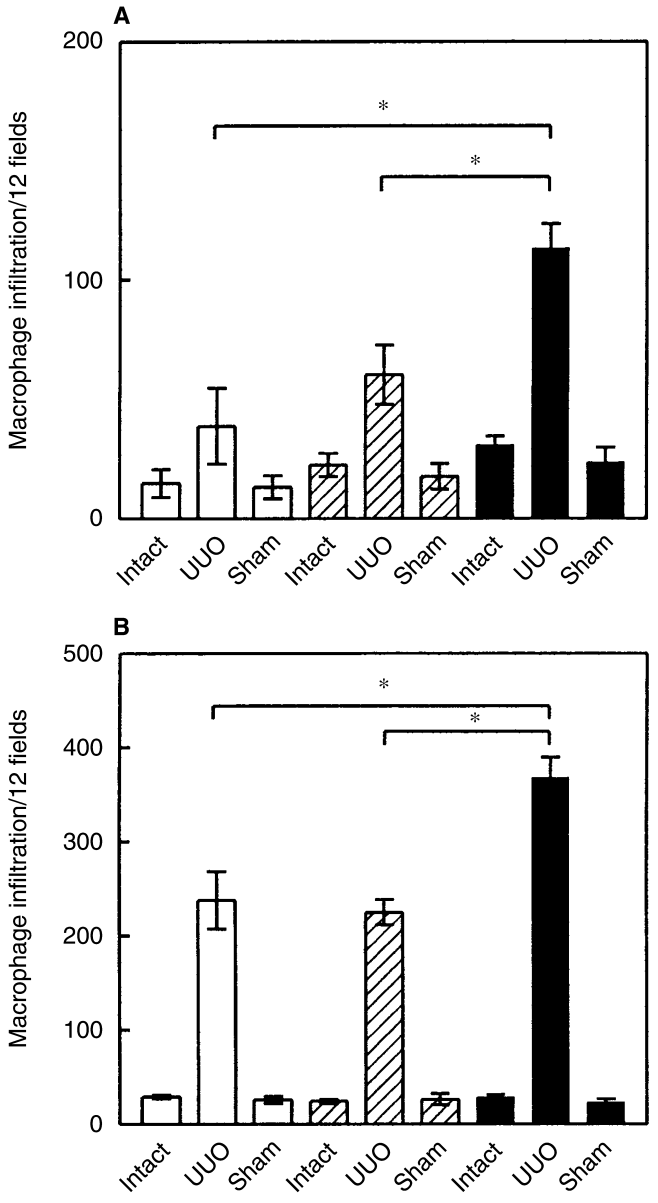

Fig. 2. Relative area of macrophage infiltration identified by F4/80 antibody five days (*A*) and twelve days (*B*) after operation. Twelve fields were analyzed at a magnification of ×400 using a grid. Abbreviations are: Intact, intact opposite kidney; UUO, obstructed kidney; Sham, sham operated control. Symbols are: (□) $EPL^{-/-}$; (▨) $L^{-/-}$; (■) wild-type; $*P < 0.05$.

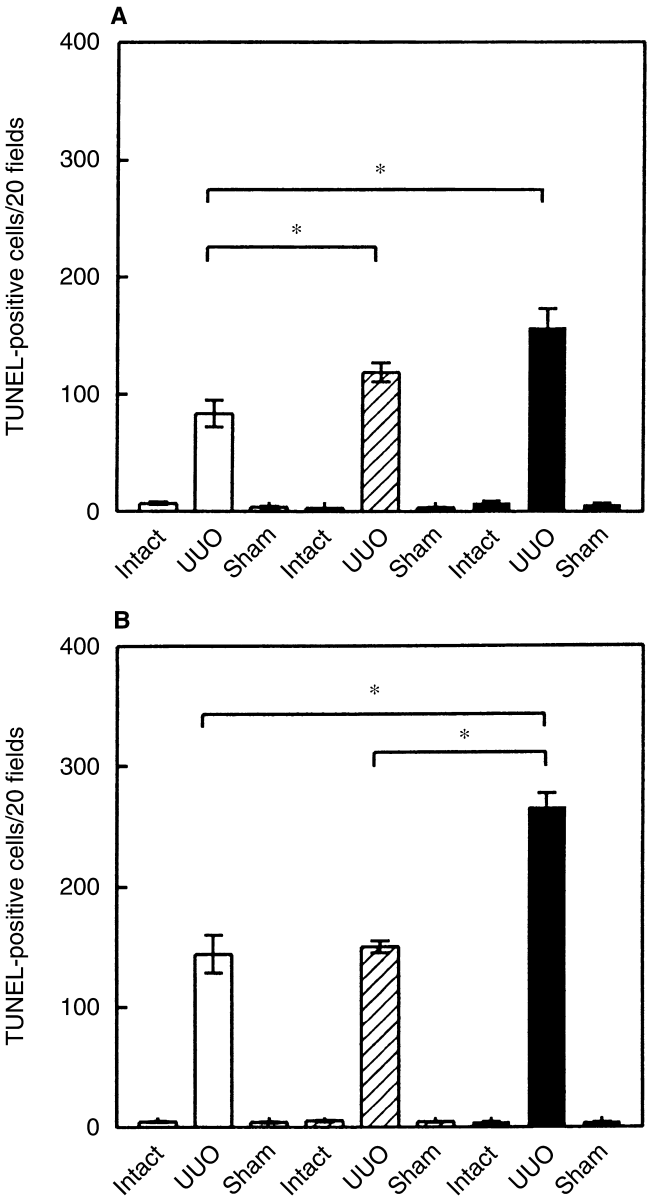

Fig. 3. Density of apoptotic tubular cells, identified by TdT uridine-nick-end label (TUNEL) technique five days (*A*) and twelve days (*B*) after operation. Twenty fields were analyzed at a magnification of ×400. Abbreviations are: Intact, intact opposite kidney; UUO, obstructed kidney; Sham, sham operated control. Symbols are: (□) $EPL^{-/-}$; (▨) $L^{-/-}$; (■) wild-type; $*P < 0.05$.

crease by 53%. Intact opposite kidneys and sham operated controls had no signs of tubular atrophy.

Interstitial fibrosis

Collagen deposition was clearly stained and confined to the renal interstitium. In obstructed kidneys of WT, $EPL^{-/-}$, and $L^{-/-}$ at 5 and 12 days after UUO, interstitial collagen was markedly increased in the interstitial space compared with intact opposite kidneys and sham operated controls (Fig. 6). The deposition of interstitial collagen in UUO was significantly less pronounced in selectin-deficient mice than in wild-type mice 12 days after surgery. $EPL^{-/-}$ showed a decrease in interstitial fibrosis by 60%, and $L^{-/-}$ demonstrated a decrease by 43% ($P < 0.001$ and $P < 0.007$, respectively). In intact opposite controls and sham-operated kidneys, there was no interstitial collagen deposition in selectin-deficient and wild-type mice at all time points studied.

DISCUSSION

This study addresses the role of selectins in tubulointerstitial renal disease induced by UUO. We show that

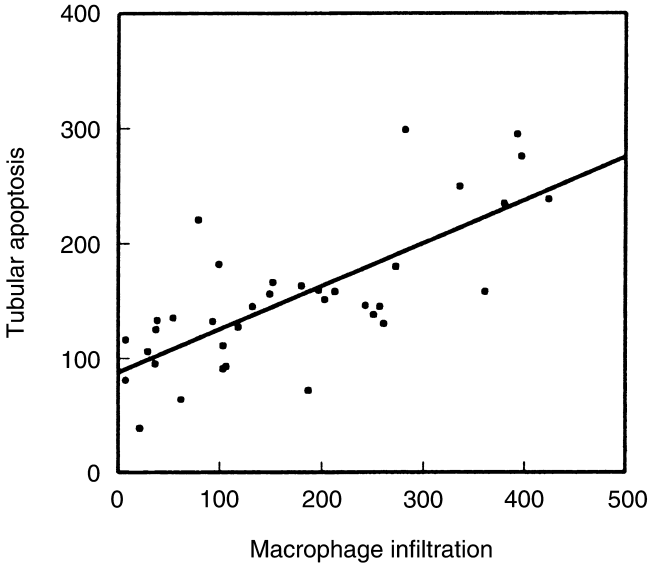

Fig. 4. Linear regression of macrophage infiltration and tubular apoptosis in obstructed kidneys of wild-type, EPL$^{-/-}$ and L$^{-/-}$ mice at day 5 and day 12 after surgery. Macrophage infiltration, identified by F4/80 antibody, was analyzed using a grid in twelve non-overlapping fields at a magnification of ×400. Apoptosis in tubular cells (TUNEL) was analyzed in twenty fields at a magnification of ×400. $r = 0.74$ and $P < 0.05$.

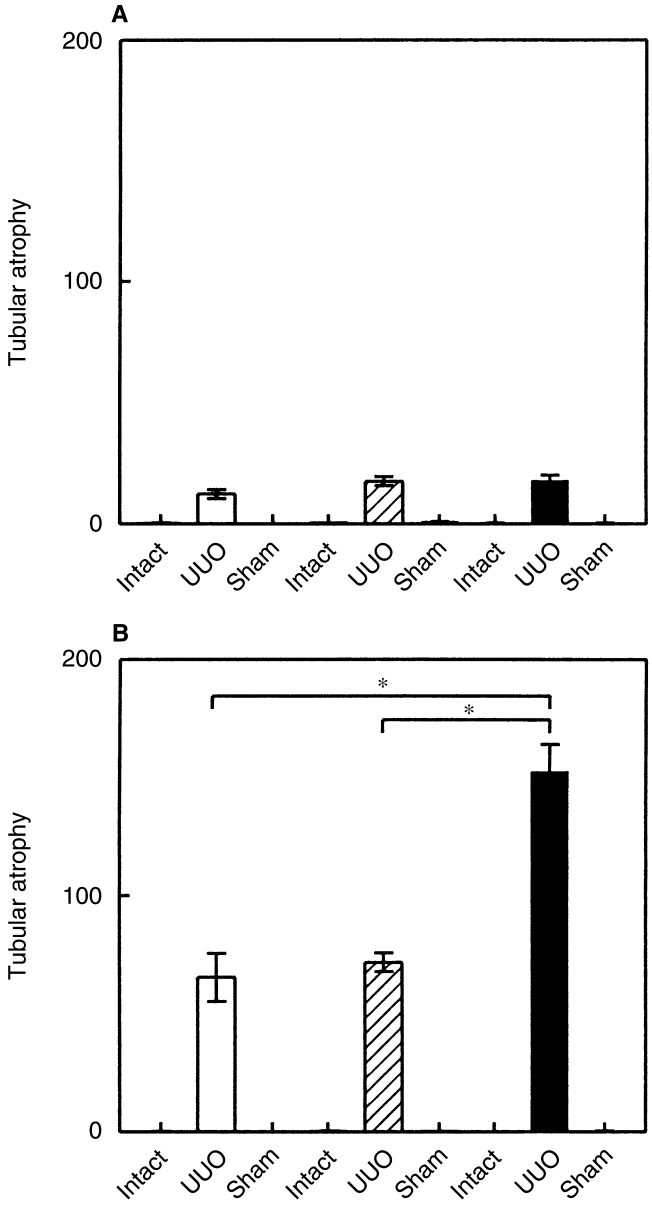

Fig. 5. Density of atrophic tubules, identified by PAS staining five days (*A*) and twelve days (*B*) after the operation. Twenty fields were analyzed at a magnification of ×400. Abbreviations are: Intact, intact opposite kidney; UUO, obstructed kidney; Sham, sham operated control. Symbols are: (□) EPL$^{-/-}$; (▨) L$^{-/-}$; (■) wild-type; *$P < 0.05$.

selectins mediated macrophage infiltration in obstructive nephropathy in newborn mice. The absence of all selectins (EPL$^{-/-}$ mice) and of L-selectin (L$^{-/-}$ mice) was associated with a marked reduction in macrophage infiltration into the tubulointerstitium compared to wild-type controls. The decrease in macrophage influx after UUO was equally pronounced in EPL$^{-/-}$ and L$^{-/-}$ mice, which is consistent with the severe impairment in leukocyte rolling and adhesion in EPL$^{-/-}$ and L$^{-/-}$ mice [19]. In the present study, L-selectin, which is constitutively expressed on most leukocytes, significantly contributed to macrophage infiltration into the obstructed kidney. This is consistent with a previous report on L-selectin and its ligands mediating macrophage influx in UUO [18]. Nevertheless, E- and P-selectin also may contribute to leukocyte recruitment in our model, because overlapping functions of the three selectins have been extensively described [19, 28, 29]. The marked decrease in interstitial macrophage infiltration in the present study cannot be explained by reduced leukocyte or monocyte counts in EPL$^{-/-}$ and L$^{-/-}$ mice, since selectin-deficient mice display varying degrees of leukocytosis [30]. Macrophage influx in our model was not exclusively dependent on selectins. In the absence of all three selectins, macrophage infiltration was reduced but not eliminated. This suggests that selectin independent pathways of leukocyte recruitment exist. Furthermore, it has been shown that other macrophage-recruiting molecules (such as MCP-1, osteopontin, ICAM-1, VCAM-1) have important roles in leukocyte recruitment after UUO [3–10]. We also show that the decrease in macrophage infiltration in selectin-deficient mice was stronger at 5 days than at 12 days after UUO, suggesting that selectins mediate predominantly early macrophage influx. In addition, since UUO is not only characterized by an increase in mononuclear cell infiltrate but also by the proliferation of interstitial cells, the observed increase in interstitial macrophage infiltration over time in all UUO kidneys may also be due to an increased macrophage proliferation in situ. Staining for proliferating nuclear antigen (PCNA) and F4/80-macrophages in serial sections did not clearly

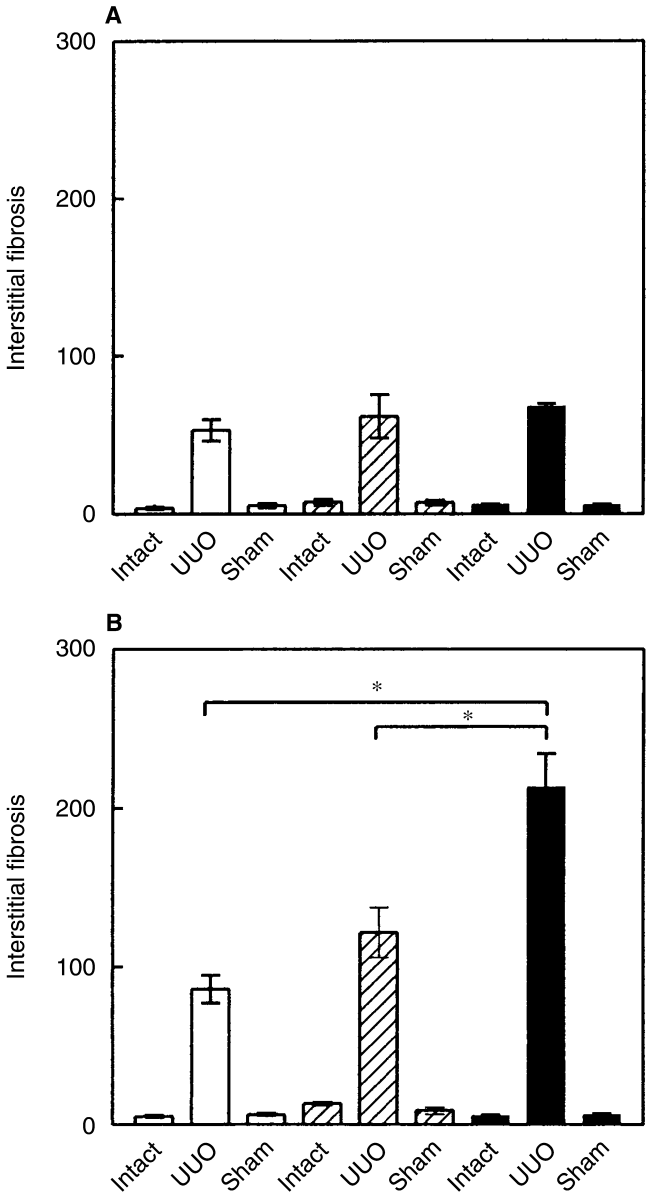

Fig. 6. Relative area of interstitial collagen, identified by Masson trichrome staining, five days (*A*) and twelve days (*B*) after the operation. Twenty fields were analyzed at a magnification of ×400. Abbreviations are: Intact, intact opposite kidney; UUO, obstructed kidney; Sham, sham operated control. Symbols are: (□) $EPL^{-/-}$; (▨) $L^{-/-}$; (■) wild-type; $^*P < 0.05$.

distinguish between proliferating macrophages and other proliferating cells in the interstitium (data not shown).

Selectins and their ligands have been shown to mediate macrophage infiltration in other models of kidney diseases. In diabetic nephropathy, the number of infiltrating macrophages correlated with the intensity of E-selectin on peritubular capillaries in the interstitium [31]. During kidney allograft rejection, which is characterized by infiltration of lymphocytes and monocytes, L-selectin ligands were induced on peritubular and venous endothelium [32]. However, in a model of accelerated nephrotoxic nephritis, mice deficient in P-selectin showed significantly greater macrophage infiltration into the interstitium than wild-type controls [33]. There are a number of parallels between the renal cellular response to transient ischemia and the response to UUO: vasoconstriction, tubular obstruction, and tubular apoptosis. In ischemia/reperfusion models of acute renal failure, E- and P-selectin have been shown to mediate leukocyte infiltration into the kidney [34, 35].

Changes in adhesion molecule expression not only affect leukocyte recruitment, but likely also the execution of certain potentially harmful effector functions during leukocyte adhesion to endothelium, interstitial cells and matrix, and tubular cells. In the present study, selectin-deficient mice with UUO demonstrated a significant reduction in tubular apoptosis compared to wild-type controls. The reduction in tubular apoptosis was greater in $EPL^{-/-}$ than in $L^{-/-}$, suggesting again that E- and P-selectin may contribute to tubular cell death after UUO. In the obstructed kidney, apoptosis was more pronounced in distal tubular cells than in proximal tubules and did not affect the glomeruli. When we correlated tubular apoptosis and macrophage infiltration in our model, we found a strong and significant relationship, suggesting that interstitial macrophages stimulate tubular apoptosis in obstructed kidneys. This novel finding suggests a possible role of activated macrophages in the development of tubular apoptosis in UUO. In our study, accumulation of F4/80 positive macrophages was predominantly noted in peritubular and interstitial areas, where tubular injury was evident. This is consistent with reports that macrophage accumulation adjacent to tubular cells correlates with tubular apoptosis and increased tubular expression of monocyte chemoattractant protein-1 (MCP-1) in nephrotoxic serum nephritis [36]. In vitro experiments suggested that macrophages can release soluble factors capable of triggering tubular cell death [36]. Conflicting data concerning macrophage infiltration and apoptosis were reported in various models of UUO. Deficiency in osteopontin, a macrophage adhesion protein, led to a decrease in macrophage infiltration after UUO, but caused an increase in interstitial and tubular apoptosis [9]. The investigators argued that the increase in apoptosis could be due to either an increase in the number of apoptotic cells, or could reflect decreased clearance of apoptotic cells due to the reduction in macrophage infiltration. However, no correlation between tubular apoptosis and macrophage infiltration was found [9]. Macrophage products such as tumor necrosis factor-α (TNF-α), transforming growth factor-β (TGF-β), reactive oxygen species, perforin, and Fas ligand have been implicated in apoptosis in other systems [37, 38].

Tubular atrophy, which most likely results from a progressive loss of tubular cells by apoptosis, was signifi-

cantly reduced in selectin-deficient mice. The reduction of tubular atrophy in $EPL^{-/-}$ and $L^{-/-}$ mice was only detectable 12 days after UUO. Prevention of macrophage infiltration in selectin-deficient mice, as shown here, inhibited tubular apoptosis and thereby preserved tubular epithelial morphology, contributing to prevention of tubular atrophy.

Interstitial fibrosis is a hallmark of obstructive nephropathy [13]. In the present study, selectin-deficient mice were markedly protected from interstitial fibrosis. The decrease in collagen deposition was likely a consequence of the reduction in macrophage infiltration in $EPL^{-/-}$ and $L^{-/-}$ mice. This observation is consistent with other studies in which reduced macrophage infiltration was associated also with diminished interstitial fibrosis [39]. Several studies have demonstrated clearly that inhibition of the renin-angiotensin system (by angiotensin converting enzyme inhibition, type 1 angiotensin II receptor blockade, or reduction of angiotensinogen gene expression) was protective against interstitial fibrosis stimulated by UUO [40–44]. Recently, it was shown that macrophage infiltration and interstitial fibrosis were reduced in mice deficient in angiotensin II type 1a receptor, suggesting a link via angiotensin-induced nuclear factor-κB (NF-κB) activation and up-regulation of macrophage adhesion molecules [45]. Prevention of macrophage influx by immunosuppressive agents also suppressed markedly fibrosis in the interstitial space [46]. The mechanism by which macrophages induce interstitial fibrosis is unknown. Macrophages produce and secrete cytotoxic substances, such as proteolytic enzymes, reactive oxygen species [5], nitric oxide, proinflammatory [interleukin-1 (IL-1), IL-6, TNF-α] and profibrogenic cytokines (TGF-β, platelet-derived growth factor). A reduction in these profibrogenic cytokines has been shown to attenuate interstitial fibrosis in UUO [47]. It also may account for the decrease in interstitial fibrosis observed in selectin-deficient mice.

In conclusion, this study demonstrates that selectins are important mediators of macrophage infiltration in UUO, leading to tubular apoptosis, tubular atrophy and interstitial fibrosis. Understanding the mechanisms underlying macrophage recruitment into the tubulointerstitium is of critical importance, because this may lead to more specific anti-inflammatory drug design. Inhibition of selectins could be an attractive approach to protect kidneys from progressive obstructive nephropathy.

ACKNOWLEDGMENTS

This research was supported in part by NIDDK 44756 grant to Dr. Chevalier. Dr. Lange-Sperandio is supported by a stipend from the German Research Foundation (DFG) La 1257/1-1, by a Children Medical Center (CMC) grant, and by the CHRC core laboratory, Charlottesville, University of Virginia. We thank Dr. Arthur Beaudet, Baylor College, Houston, for providing E-selectin/P-selectin/L-selectin triple-deficient mice, Dr. Thomas F. Tedder, Duke University, for providing L-selectin deficient mice, and Dr. Klaus Ley, University of Virginia, for providing murine breeding pairs.

Reprint requests to Robert L. Chevalier, M.D., Department of Pediatrics, P.O. Box 800386, University of Virginia, Health Sciences Center, Charlottesville, Virginia 22908-0386, USA.
E-mail: rlc2m@virginia.edu

REFERENCES

1. Fivush BA, Jabs K, Neu AM, *et al*: Chronic renal insufficiency in children and adolescents: The 1996 annual report of NAPRTCS. *Pediatr Nephrol* 12:328–337, 1998
2. Chevalier RL: Molecular and cellular pathophysiology of obstructive nephropathy. *Pediatr Nephrol* 13:612–619, 1999
3. Diamond JR, Kees-Folts D, Ding G, *et al*: Macrophages, monocyte chemoattractant peptide-1 and TGFβ in experimental hydronephrosis. *Am J Physiol* 266:F292–F303, 1994
4. Diamond JR: Macrophages and progressive renal disease in experimental hydronephrosis. *Am J Kidney Dis* 26:133–140, 1995
5. Ricardo SD, Diamond JR: The role of macrophages and reactive oxygen species in experimental hydronephrosis. *Semin Nephrol* 18:612–621, 1998
6. Klahr S: Urinary tract obstruction. *Semin Nephrol* 21:133–145, 2001
7. Morrissey JJ, Klahr S: Differential effects of ACE and AT1 receptor inhibition on chemoattractant and adhesion molecule synthesis. *Am J Physiol* 274:F580–F586, 1998
8. Shappell SB, Mendoza LH, Gurpinar T, *et al*: Expression of adhesion molecules in kidney with experimental chronic obstructive nephropathy: The pathogenic role of ICAM-1 and VCAM-1. *Nephron* 85:156–166, 2000
9. Ophascharoensuk V, Giachelli CM, Gordon K, *et al*: Obstructive uropathy in the mouse: Role of osteopontin in interstitial fibrosis and apoptosis. *Kidney Int* 56:571–580, 1999
10. Taal MW, Zandi-Nejad K, Weening B, *et al*: Proinflammatory gene expression and macrophage recruitment in the rat remnant kidney. *Kidney Int* 58:1664–1676, 2000
11. Schreiner GF, Harris KPG, Purkerson ML, *et al*: Immunological aspects of acute ureteral obstruction: Immune cell infiltrate in the kidney. *Kidney Int* 34:487–493, 1988
12. Rovin BH, Harris KP, Morrison A, *et al*: Renal cortical release of a specific macrophage chemoattractant in response to ureteral obstruction. *Lab Invest* 63:213–220, 1990
13. Diamond JR, Ricardo SD, Klahr S: Mechanisms of interstitial fibrosis in obstructive nephropathy. *Semin Nephrol* 18:612–621, 1998
14. Shappell SB, Gurpinar T, Lechago J, *et al*: Chronic obstructive uropathy in severe combined immunodeficient (SCID) mice: Lymphocyte infiltration is not required for progressive tubulointerstitial injury. *J Am Soc Nephrol* 9:1008–1017, 1998
15. Vestweber D: *The Selectins*. Amsterdam, Harwood Academic Publishers, 1997, pp 1–225
16. Butcher EC: Leukocyte-endothelial-cell recognition: Three (or more) steps to specificity and diversity. *Cell* 67:1033–1036, 1991
17. Springer TA: Traffic signals for lymphocyte recirculation and leukocyte emigration: The multistep paradigm. *Cell* 76:301–314, 1994
18. Shikata K, Suzuki Y, Wada J, *et al*: L-selectin and its ligands mediate infiltration of mononuclear cells into kidney interstitium after ureteric obstruction. *J Pathol* 188:93–99, 1999
19. Jung U, Ley K: Mice lacking two or all three selectins demonstrate overlapping and distinct functions for each selectin. *J Immunol* 162:6755–6762, 1999
20. Tedder TF, Steeber DA, Pizcueta P: L-selectin-deficient mice have impaired leukocyte recruitment into inflammatory sites. *J Exp Med* 181:2259–2264, 1995
21. Ley K: Gene-targeted mice in leukocyte adhesion research. *Microcirculation* 2:141–150, 1995
22. Ley K, Bullard DC, Arbones ML, *et al*: Sequential contribution of L- and P-selectin to leukocyte rolling in vivo. *J Exp Med* 181:679–675, 1995
23. Collins RG, Jung U, Ramirez M, *et al*: The dermal and pulmonary inflammatory disease in E/P-selectin double null mice is reduced in triple selectin null mice. *Blood* 98:727–735, 2001

24. Hughes J, Brown P, Shankland SJ: Cyclin kinase inhibitor $p21^{CIP/WAF1}$ limits interstitial cell proliferation following ureteric obstruction. *Am J Physiol* 277:F948–F956, 1999
25. Chevalier RL, Goyal S, Wolstenholme JT, Thornhill BA: Obstructive nephropathy in the neonate is attenuated by epidermal growth factor. *Kidney Int* 54:38–47, 1998
26. Chevalier RL, Thornhill BA, Wolstenholme JT, Kim A: Unilateral ureteral obstruction in early development alters renal growth: dependence on the duration of obstruction. *J Urol* 161:399–313, 1999
27. Chevalier RL, Thornhill BA, Chang AY: Unilateral ureteral obstruction in neonatal rats leads to renal insufficiency in adulthood. *Kidney Int* 58:1987–1995, 2000
28. Bosse R, Vestweber D: Only simultaneous blocking of the L- and P-selectin completely inhibits neutrophil migration into mouse peritoneum. *Eur J Immunol* 24:3019–3024, 1994
29. Davenpeck KL, Steeber DA, Tedder TF, Bochner BS: P- and L-selectin mediate distinct but overlapping functions in endotoxin-induced leukocyte-endothelial interactions in the rat mesenteric microcirculation. *J Immunol* 159:1977–1986, 1997
30. Robinson SD, Frenette PS, Rayburn H, *et al*: Multiple, targeted deficiencies in selectins reveal a predominant role for P-selectin in leukocyte recruitment. *Proc Natl Acad Sci USA* 96: 11452–11457, 1999
31. Hirata K, Shikata K, Matsuda M, *et al*: Increased expression of selectins in kidneys of patients with diabetic nephropathy. *Diabetologica* 41:185–192, 1998
32. Kirveskari J, Paavonen T, Häyry P, Renkonen R: De novo induction of endothelial L-selectin ligands during kidney allograft rejection. *J Am Soc Nephrol* 11:2358–2365, 2000
33. Rosenkranz AR, Mendrick DL, Cotran RS, Mayadas TN: P-selectin deficiency exacerbates experimental glomerulonephritis: A protective role for endothelial P-selectin in inflammation. *J Clin Invest* 103:649–659, 1999
34. Singbartl K, Green SA, Ley K: Blocking P-selectin protects from ischemia/reperfusion-induced acute renal failure. *FASEB J* 14:48–54, 2000
35. Singbartl K, Ley K: Protection from ischemia/reperfusion induced severe acute renal failure by blocking E-selectin. *Crit Care Med* 28:2507–2514, 2000
36. Tesch GH, Schwarting A, Kinoshita K, *et al*: Monocyte chemoattractant protein-1 promotes macrophage-mediated tubular injury, but not glomerular injury, in nephrotoxic serum nephritis. *J Clin Invest* 103:73–80, 1999
37. Savill J: Apoptosis in the kidney. *J Am Soc Nephrol* 5:12–21, 1994
38. Nagata S, Golstein P: The Fas death factor. *Science* 267:1449–1456, 1995
39. Hruska KA, Guo G, Wozniak M, *et al*: Osteogenic protein-1 prevents renal fibrogenesis associated with ureteral obstruction. *Am J Physiol* 280:F130–F143, 2000
40. Fern RJ, Yesko CM, Thornhill BA, *et al*: Reduced angiotensinogen expression attenuates renal interstitial fibrosis in obstructive nephropathy in mice. *J Clin Invest* 103:39–46, 1999
41. Chung KH, Gomez RA, Chevalier RL: Regulation of renal growth factors and clusterin by AT1 receptors during neonatal ureteral obstruction. *Am J Physiol* 268:F1117–F1123, 1995
42. Ishidoya S, Morrissey J, Mc Cracken R, *et al*: Angiotensin II receptor antagonist ameliorates renal tubulointerstitial fibrosis caused by unilateral ureteral obstruction. *Kidney Int* 47:1285–1294, 1995
43. Ishidoya S, Morrissey J, Mc Cracken R, Klahr S: Delayed treatment with enalapril halts tubulointerstitial fibrosis in rats with obstructive nephropathy. *Kidney Int* 49:1110–1119, 1996
44. Kaneto H, Morrissey J, McCracken R, *et al*: Enalapril reduces collagen type IV synthesis and expansion of the interstitium in the obstructed rat kidney. *Kidney Int* 45:1637–1647, 1994
45. Satoh M, Kashihara N, Yamasaki Y, *et al*: Renal interstitial fibrosis is reduced in angiotensin II type 1a receptor-deficient mice. *J Am Soc Nephrol* 12:317–325, 2001
46. Sakai T, Kawamura T, Shirasawa T: Mizoribine improves renal tubulointerstitial fibrosis in unilateral ureteral obstruction (UUO)-treated rat by inhibiting the infiltration of macrophages and the expression of α-smooth muscle actin. *J Urol* 158:2316–2322, 1997
47. Ludewig D, Kosmehl H, Sommer M, *et al*: PDGF receptor kinase blocker AG1295 attenuates interstitial fibrosis in the rat kidney after unilateral obstruction. *Cell Tissue Res* 299:97–103, 2000